TRANSACTIONS ON EMERGING TELECOMMUNICATIONS TECHNOLOGIES
Trans. Emerging Tel. Tech. (2015)
Published online in Wiley Online Library (wileyonlinelibrary.com). DOI: 10.1002/ett.2968

RESEARCH ARTICLE

Backhaul aware joint uplink and downlink user association for delay-power trade-offs in HetNets with hybrid energy sources

Dantong Liu[1]*, Yue Chen[1], Kok Keong Chai[1] and Tiankui Zhang[2]

[1] School of Electronic Engineering and Computer Science, Queen Mary University of London, London E1 4NS, UK
[2] School of Information and Communications Engineering, Beijing University of Posts and Telecommunications, Beijing, China

ABSTRACT

In cellular networks, conventional user association algorithms are solely based on downlink (DL) performance, which may lead to inefficient transmission power and high interference in the uplink (UL) transmission. In addition, the backhaul data rate constraint has been neglected by the majority of the existing user association algorithms. However, the backhaul constraint has become more severe in heterogeneous networks (HetNets) where small cells are densely deployed to meet the skyrocketing data traffic demand. In this paper, we propose an optimal backhaul-aware joint UL and DL user association for delay-power trade-offs in HetNets with hybrid energy sources. In the considered HetNets, all the base stations are assumed to be powered by a combination of power grid and renewable energy sources, in order to achieve both uninterrupted and green communications. Taking both UL and DL transmissions into consideration, the proposed user association algorithm aims to improve network quality of service by minimising the sum of UL and DL average traffic delay, as well as to reduce the overall UL power consumption of users and DL on-grid power consumption by maximising the utilisation of green power harvested from renewable energy sources. To this end, a convex optimisation problem is formulated to minimise the weighted sum of cost of average traffic delay and cost of power consumption. We have proved that the proposed user association algorithm converges to the global optimum, which enables a flexible trade-off between average traffic delay and power consumption. Simulation results validate the effectiveness of the proposed algorithm in adapting the traffic loads among base stations along with the distribution of green power and the backhaul data rate constraint. Simulation results also demonstrate that the proposed user association algorithm achieves prominent improvement in UL average traffic delay reduction and effectively reduces both the DL on-grid power consumption and overall UL power consumption of users, with limited sacrifice on DL average traffic delay, compared with the user association algorithm only based on DL performance. Copyright © 2015 John Wiley & Sons, Ltd.

***Correspondence**
D. Liu, School of Electronic Engineering and Computer Science, Queen Mary University of London, London E1 4NS, UK.
E-mail: d.liu@qmul.ac.uk

Received 22 April 2015; Revised 12 June 2015; Accepted 27 June 2015

1. INTRODUCTION

The emerging fifth-generation (5G) mobile networks expect significantly higher transmission rate and energy efficiency. Heterogeneous networks (HetNets), where various low-power base stations (BSs) are underlaid in a macrocellular network, are able to achieve more spectrum-efficient and energy-efficient communications [1] to meet the requirements of 5G networks.

Driven by environmental concerns and regulatory pressure, green communication has drawn tremendous attention from both industry and academia. Energy harvesting is appealing because BSs are capable of harvesting energy from the renewable energy sources, such as solar panels and wind turbines, thereby substantially reducing the overall energy consumption throughout the network. Yet, although the amount of renewable energy is potentially unlimited, the intermittent nature of the energy from renewable energy sources will result in highly random energy availability in BSs. Hence, in practice, BSs powered by hybrid energy sources, a combination of power grid and renewable energy sources, are much more practical than those solely powered by renewable energy sources in order to provide uninterrupted service [2]. In the literature, power allocation [3], coordinated multi-input multi-output [4],

network planning [5] and green energy allocation [6] have been studied in the hybrid energy sources-powered scenario.

User association, which refers to associating user with a proper serving BS, has a great impact on the performance of wireless networks. Most of the research works on user association investigate the problem from either the downlink (DL) [7–9] or uplink (UL) [10, 11] perspective. It is worth mentioning that HetNets introduce a major asymmetry between the UL and DL in terms of channel, traffic and hardware limitation. Because of the UL–DL asymmetry in HetNets, the user association for the optimal DL or UL performance only will not be effective to the opposite direction. Specifically, we take the conventional user association policy as an example, where a user is associated with the BS from which it receives the strongest DL reference signal received power (RSRP) [12]. As illustrated in Figure 1, user A is located in the vicinity of a pico BS (PBS). Despite the distance from user A to the PBS is shorter than that from user A to the macro-BS (MBS), user A is associated with MBS due to the stronger received RSRP from the MBS. In the UL, user A needs to transmit with high power to ensure the target signal-to-noise ratio received by the MBS. This will introduce high UL interference to users in the picocell, thereby degrading both the spectrum and energy efficiencies and shortening users battery life.

In this sense, it is imperative to take both the UL and DL performances into consideration when making user association decision in HetNets. To the best of our knowledge, only a limited number of existing works have considered the joint UL and DL user association in HetNets [13, 14]. In [13], a user association algorithm was proposed to maximise both UL and DL energy efficiencies via Nash bargain solution. In [14], a user association and beamforming design were proposed to coordinate the interference for energy minimisation.

In addition, all the aforementioned discussions imply that the network has perfect backhaul between the BS and the network controller, and the wireless access link between the BS and the user is the network bottleneck. This implication is generally correct for the well-planned MBS. However, in HetNets, the potentially dense deployed small BSs may incur overwhelming traffic over backhaul link. On the other hand, the current small cell backhaul solutions, such as xDSL, non-line-of-sight microwave, are far from the ideal backhaul solution with sufficiently large data rate [15]. As such, the backhaul data rate constraint has become far more stringent in HetNets.

To cope with the foregoing issues, we propose an optimal backhaul-aware joint UL and DL user association for delay-power trade-offs in HetNets with hybrid energy sources in this paper. Average traffic delay is a critical metric for user association, which has been widely used in the existing research [7, 16–19]. The delay that we considered here includes not only the DL and UL average traffic delay over the wireless access link between the BS and the user but also the DL and UL average traffic delay over the backhaul link between the BS and the network controller. The power grid operation is costly and non-environmentally friendly. In contrast, the harvested energy from renewable energy source is green, sustainable and free of cost. Thus, instead of the overall DL network power consumption minimisation, we try to reduce DL on-grid power consumption by maximising the utilisation of green power harvested from renewable energy sources. As such, for the power consumption, we take both the DL on-grid power consumption and overall UL power consumption of users into account. In wireless networks, power saving is often achieved at the price of degradation in network quality of service (QoS) (i.e. higher latency and lower throughput) [20]. With this in mind, the proposed user association algorithm aims to achieve a flexible trade-off between UL/DL average traffic delay and UL/DL power consumption. To this end, a convex optimisation problem is formulated to minimise the weighted sum of cost of average traffic delay and cost of power consumption. We prove that the proposed user association algorithm converges to the global optimum.

This paper is organised as follows. Section 2 gives the system model. Section 3 formulates problem. Section 4 presents the proposed user association algorithm and the properties of the proposed algorithm. Sections 5 and 6 are simulations and conclusions, respectively.

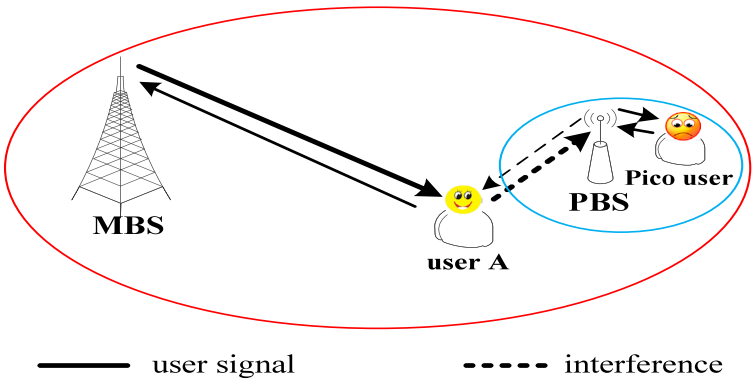

Figure 1. Downlink reference signal received power-based user association causes severe uplink interference. BS, base station; MBS, macro BS; PBS, pico BS.

2. SYSTEM MODEL

We focus on a two-tier HetNet where tier 1 is modelled as macrocell and tier 2 as picocell. MBSs provide basic coverage, whereas PBSs are deployed in the coverage area of each MBS to enhance capacity. All the BSs are assumed to be powered by both the power grid and renewable energy sources. The proposed user association algorithm is carried out within a macrocell geographical area $\mathcal{L} \subset \mathbb{R}^2$, which is served by a set of BSs $\mathcal{B}$ including one MBS and several PBSs, where all the BSs are assumed to share the same frequency band with frequency reuse factor equalling to one. We investigate the backhaul-constrained HetNets in this paper, and both the formulated UL and DL transmissions are composed of the wireless access link between the BS and the user, and the backhaul link between the network controller and the BS. Let $x \in \mathcal{L}$ denote a location and $i \in \mathcal{B}$ an index ith BS, where $i = 1$ indicates the MBS and others are PBSs. Then the proposed user association algorithm is applied to decide which BS within $\mathcal{L}$ will serve which user at location x. Figure 2 details the system model for the proposed backhaul-aware joint UL and DL user association in HetNets with hybrid energy sources.

We assume that each user has both UL and DL transmission requests during the period when associated with certain BS. There are two main techniques to separate UL and DL transmissions on the same physical transmission medium: the time-division duplex (TDD) and frequency-division duplex. TDD system, with the advantages to accommodate UL and DL traffic asymmetrically, has been regarded as a promising paradigm in 5G networks. Thus, in the paper, we use TDD to separate the DL and UL transmissions with the synchronous operation across the entire network to eliminate BS-to-BS and user-to-user interference [21]. As an inherit feature of TDD system, channel reciprocity is adopted here, where the UL and DL channels between the same communicating pairs have the same channel gain. We assume that the traffic requests arrive according to an inhomogeneous Poisson point process with the arrival rate per unit area $\lambda(x)$, and the UL and DL traffic sizes are independently distributed with mean $\upsilon(x)$ and $\mu(x)$, respectively.

In order to formulate the user association problem, we define the user association indicator as $y_i(x)$. If the user at location x is associated with BS i, $y_i(x) = 1$; otherwise, $y_i(x) = 0$. We assume that at each time, one user can only associate with one BS, and thus, we have $\sum_{i\in\mathcal{B}} y_i(x) = 1$. For the sake of decoupling the association and scheduling problem, we assume that all the users associated with the same BS are severed in a round robin fashion. To facilitate the subsequent analysis, we define $\boldsymbol{y} = \{\boldsymbol{y}_i | i \in \mathcal{B}\}$, where $\boldsymbol{y}_i = \{y_i(x) | y_i(x) = \{0, 1\}, x \in \mathcal{L}\}$.

2.1. Traffic model

2.1.1. Uplink traffic model.

During the UL open-loop control, χ is set as the target signal-to-noise ratio at BS. Thus, the desired transmission power of user at location x when associated with BS i is given by

$$p_i^u(x) = \min\left\{\chi\sigma^2 \Big/ g_i(x), p_{\max}^u(x)\right\} \tag{1}$$

where σ^2 is the noise power level, $p_{\max}^u(x)$ is user's maximum transmission power and $g_i(x)$ is the channel gain between the user at location x and BS i, which includes pathloss and shadowing.

Assuming that a mobile user at location x is associated with BS i, the UL transmission rate $r_i^u(x)$ from this user to BS i can be generally expressed according to Shannon–Hartley theorem [17], with W denoted as the operating bandwidth:

$$r_i^u(x) = W\log_2\left(1 + \gamma_i^u(x)\right) \tag{2}$$

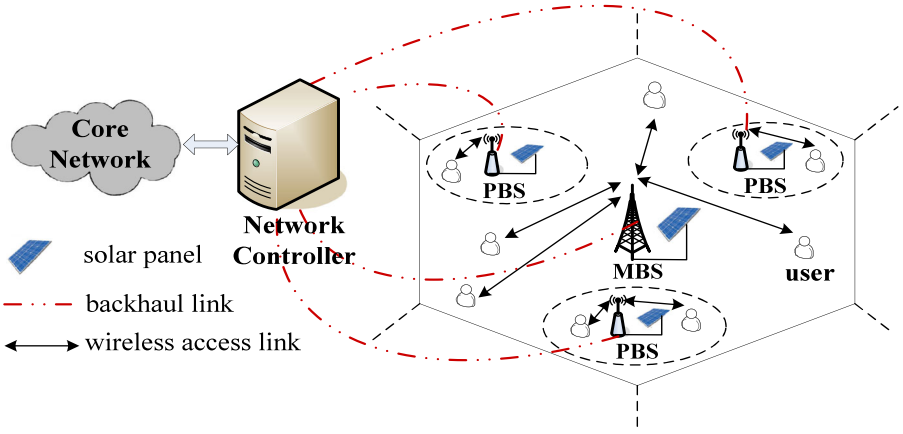

Figure 2. System model for the proposed backhaul-aware joint UL and DL user association in HetNets with hybrid energy sources. BS, base station; MBS, macro BS; PBS, pico BS.

where

$$\gamma_i^u(x) = \frac{p_i^u(x) g_i(x)}{I_i(x) + \sigma^2} \tag{3}$$

here, $I_i(x)$ is the average interference to the UL transmission of the user at location x from all the other users in neighbouring cells. Note that fast fading is not considered here because the time scale of user association is much larger than the time scale of fast fading. As such, $r_i^u(x)$ can be considered as a time-averaged transmission rate [16]. In the UL, the co-channel interference for a certain user comes from the users that simultaneously use the same resource block in the neighbouring cells. In reality, the users that cause interference change from one scheduling cycle to another due to scheduling dynamics. However, in terms of user association, the average interference to a user is more critical than the instantaneous interference at each scheduling cycle. Thus, we focus on the average interference to a user $I_i(x)$, which is given by [22]:

$$I_i(x) = \sum_{j \in \mathcal{B}, j \neq i} \int_{\mathcal{L} \setminus x} \left(\frac{p_j^u(\hat{x})\, y_j(\hat{x})}{N_j} \right) g_i(\hat{x})\, d\hat{x} \tag{4}$$

where $N_j = \int_{\mathcal{L} \setminus x} y_j(\hat{x})\, d\hat{x}$ is the number of users associated with BS j.

In order to guarantee the QoS of users in a sense that all the users are served with the required traffic amount, the fraction of resource blocks used by the user at location x for UL transmission, when associated with BS i, is

$$\varrho_i^u(x) = \frac{\lambda(x) \upsilon(x) y_i(x)}{r_i^u(x)} \tag{5}$$

where $\varrho_i^u(x)$ also denotes the average UL traffic load density at location x of BS i.

Based on the UL traffic load density, the UL traffic load of BS i is given by

$$\rho_i^u = \int_{\mathcal{L}} \varrho_i^u(x) dx \tag{6}$$

According to Burke's theorem, the traffic request departure process at BS's wireless access link is a Poisson process with average departure rate equalling to the average arrival rate. Thus, the average traffic arrival rate in BS's backhaul is $\lambda(x)$.

We assume that the expected backhaul data rate is constant during the user association period [23]. With R_i^u denoted as the UL backhaul data rate of BS i, the average UL backhaul traffic load density at location x of BS i is expressed as follows:

$$\tilde{\varrho}_i^u(x) = \frac{\lambda(x) \upsilon(x) y_i(x)}{R_i^u} \tag{7}$$

Then the UL backhaul traffic load of BS i is given by

$$\tilde{\rho}_i^u = \int_{\mathcal{L}} \tilde{\varrho}_i^u(x) dx \tag{8}$$

2.1.2. Downlink traffic model.

Assuming that a mobile user at location x is associated with BS i, the DL transmission rate from BS i to this user $r_i^d(x)$ is

$$r_i^d(x) = W \log_2 \left(1 + \gamma_i^d(x)\right) \tag{9}$$

where

$$\gamma_i^d(x) = \frac{p_i g_i(x)}{\sum_{k \in \mathcal{B}, k \neq i} p_k g_k(x) + \sigma^2} \tag{10}$$

here, p_i is the transmission power of BS i and $g_i(x)$ is the channel gain between BS i and the user at location x.

Then the average DL traffic load density at location x of BS i is derived as follows:

$$\varrho_i^d(x) = \frac{\lambda(x) \mu(x) y_i(x)}{r_i^d(x)} \tag{11}$$

Based on the DL traffic load density, the DL traffic load of BS i is given by

$$\rho_i^d = \int_{\mathcal{L}} \varrho_i^d(x) dx \tag{12}$$

Similarly, with R_i^d denoted as the DL backhaul data rate of BS i, the average DL backhaul traffic load density at location x of BS i is

$$\tilde{\varrho}_i^d(x) = \frac{\lambda(x) \mu(x) y_i(x)}{R_i^d} \tag{13}$$

And then the DL backhaul traffic load of BS i is expressed as follows:

$$\tilde{\rho}_i^d = \int_{\mathcal{L}} \tilde{\varrho}_i^d(x) dx \tag{14}$$

As such, the set $\mathcal{F}$ of the feasible user association $\boldsymbol{y}$ is given by

$$\begin{aligned} \mathcal{F} = \{ \boldsymbol{y} \,|\, & 0 \leqslant \rho_i^d \leqslant 1 - \varepsilon, 0 \leqslant \tilde{\rho}_i^d \leqslant 1 - \varepsilon, \\ & 0 \leqslant \rho_i^u \leqslant 1 - \varepsilon, 0 \leqslant \tilde{\rho}_i^u \leqslant 1 - \varepsilon, \\ & \textstyle\sum_{i \in \mathcal{B}} y_i(x) = 1, y_i(x) \in \{0, 1\}, \forall i, \forall x \} \end{aligned} \tag{15}$$

where ε is an arbitrarily small positive constant to ensure $\rho_i^d < 1$, $\tilde{\rho}_i^d < 1$, $\rho_i^u < 1$ and $\tilde{\rho}_i^u < 1$.

2.2. Power consumption model

The considered power consumption in this paper comprises the on-grid power consumed by all the BSs in DL transmission and the overall power consumption of users in UL transmission.

2.2.1. Downlink power consumption model.

We assume that both MBSs and PBSs in the HetNets are powered by hybrid energy sources: power grid and renewable energy sources. If the green power harvested from renewable energy sources is not sufficient, BSs will

consume the power from power grid. Because of the disadvantage of 'banking' green power [24], here we assume that the green power cannot be stored.

Generally, BSs consist of two types of power consumptions: static power consumption and adaptive power consumption. Adaptive power consumption is nearly linear to the loads of BSs [25]. The static power consumption is mainly caused by real-time A/D and D/A processing, air conditioning and so on, which is independent with traffic load. For the sake of energy saving, some BSs can be switched into sleep mode with negligible power consumption [†].

Here, we adopt the linear approximation in [25] to model the BS power consumption when this BS is switched into active mode, with P_i denoted as the total power consumption of BS i:

$$P_i = \Delta_i \rho_i^d p_i + P_i^s \tag{16}$$

where Δ_i is the slope of load-dependent power consumption of BS i, ρ_i^d is the DL traffic load of BS i, and p_i and P_i^s are the transmission power and static power consumption of BS i, respectively. It is worthwhile mentioning that the small BSs such as PBSs and femto BSs may have smaller static power consumptions than those of MBSs because they have neither big power amplifiers nor cooling equipments.

Then we denote P_i^g as the green power of BS i harvested from renewable energy sources, and the DL on-grid power consumption of BS i is expressed as follows:

$$P_i^{grid} = \max\left(P_i - P_i^g, 0\right) \tag{17}$$

2.2.2. Uplink power consumption model.

The UL power consumption of user at location x is determined by

$$p^u(x) = \sum\nolimits_{i\in\mathcal{B}} p_i^u(x)\varrho_i^u(x) \tag{18}$$

Then the overall UL power consumption of users in the HetNets area is

$$P^u = \int_{\mathcal{L}} p^u(x)dx \tag{19}$$

3. PROBLEM FORMULATION

We formulate the user association problem as a convex optimisation problem, which aims to reduce overall UL power consumption of users, and achieve DL on-grid power saving by optimising the utilisation of green power harvested from renewable energy sources, as well as enhance network QoS by minimising UL and DL average traffic delay. Our problem is to find optimal user association $\boldsymbol{y}$ that minimises the total system cost, which is given by

$$\min_{\boldsymbol{y}} \left\{ f(\boldsymbol{y}) = \varphi(\boldsymbol{y}) + \omega\left(\phi^d(\boldsymbol{y}) + \omega_p \phi^u(\boldsymbol{y})\right) | \boldsymbol{y} \in \mathcal{F} \right\} \tag{20}$$

where $\varphi(\boldsymbol{y})$ is the cost of average traffic delay, $\phi^d(\boldsymbol{y})$ is the cost of DL on-grid power consumption and $\phi^u(\boldsymbol{y})$ is the cost of overall UL power consumption of users. $\omega \geqslant 0$ is the relative weight to balance the trade-off between average traffic delay and power consumption. Larger ω will lead to more emphasis on the power consumption to reduce both the DL on-grid power consumption and UL power consumption of all users, while smaller ω will attach more importance to network QoS in order to decrease both UL and DL average traffic delays. ω_p is the relative weight between DL on-grid power consumption and UL power consumption of all users. Compared with the BS, the end user generally has more limited power supply. As such, we normally set $\omega_p > 1$ to pay more attention on UL power saving of all users.

3.1. Cost function of average traffic delay

We define the cost function of average traffic delay as the sum of DL wireless access delay τ_i^d, DL backhaul delay $\tilde{\tau}_i^d$, UL wireless access delay τ_i^u and UL backhaul delay $\tilde{\tau}_i^u$, which is given by

$$\varphi(\boldsymbol{y}) = \sum_{i\in\mathcal{B}} \left(\tau_i^d\left(\rho_i^d\right) + \tilde{\tau}_i^d\left(\tilde{\rho}_i^d\right) + \tau_i^u\left(\rho_i^u\right) + \tilde{\tau}_i^u\left(\tilde{\rho}_i^u\right)\right) \tag{21}$$

where $\tau_i^d\left(\rho_i^d\right) = \rho_i^d \big/ \left(1-\rho_i^d\right)$, $\tilde{\tau}_i^d\left(\tilde{\rho}_i^d\right) = \tilde{\rho}_i^d \big/ \left(1-\tilde{\rho}_i^d\right)$, $\tau_i^u\left(\rho_i^u\right) = \rho_i^u \big/ \left(1-\rho_i^u\right)$ and $\tilde{\tau}_i^u\left(\tilde{\rho}_i^u\right) = \tilde{\rho}_i^u \big/ \left(1-\tilde{\rho}_i^u\right)$.

Because users associated with the same BS are assumed to be served on a round robin fashion, when we consider the system as M/GI/1 multi-class processor sharing system in [26], $\rho_i^d \big/ \left(1-\rho_i^d\right)$ is equal to the average number of DL flows at BS i to be transmitted to users. According to Little's law, minimising the average number of flows is equivalent to minimising the average delay experienced by a typical traffic flow. Similarly, $\tilde{\tau}_i^d\left(\tilde{\rho}_i^d\right)$, $\tau_i^u\left(\rho_i^u\right)$ and $\tilde{\tau}_i^u\left(\tilde{\rho}_i^u\right)$ are modelled as average number of DL flows at BS i's backhaul, average number of UL flows at BS i from users and average number of UL flows at BS i's backhaul, respectively.

3.2. Cost function of power consumption

We define the green traffic load as the maximum DL traffic load that can be supported by the green power harvested from renewable energy sources. Based on Equation (17), the green traffic load of BS i is derived as follows:

[†]It is assumed that when the BS is in sleep mode, it acts as a passive node and listens to the pilot transmission from users for channel estimation, which consumes negligible power consumption compared with being in active mode with data transmission. It is further assumed that BS can switch between active and sleep modes frequently [14].

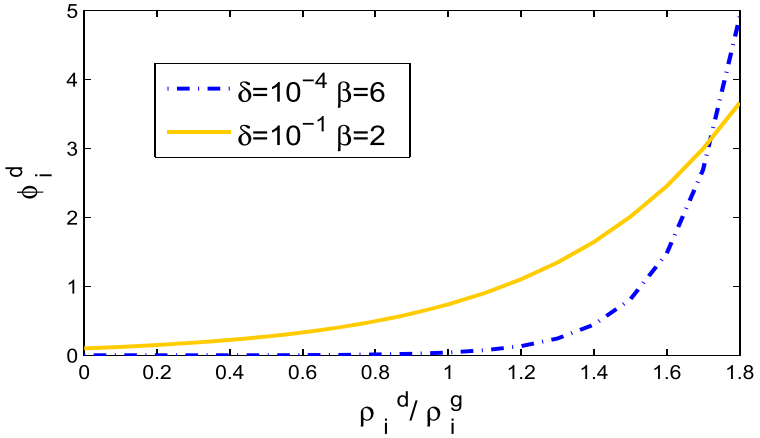

Figure 3. Cost of downlink on-grid power consumption with different values of β and δ.

$$\rho_i^g = \max\left(\varepsilon, \min\left(\frac{P_i^g - P_i^s}{\Delta_i p_i}, 1-\varepsilon\right)\right) \quad (22)$$

note that ε is an arbitrarily small positive constant to ensure $0 < \rho_i^g < 1$.

According to Equation (17), DL on-grid power is only consumed when green power is not sufficient. Thus, when the DL traffic load of BS i exceeds the amount of green traffic load, that is, $\rho_i^d > \rho_i^g$, DL on-grid power will be consumed, which leads to the increase in the cost of DL on-grid power consumption. Otherwise, the cost of DL on-grid power consumption will stay trivial. In doing so, the cost function of DL on-grid power consumption is designed as follows:

$$\phi^d(\boldsymbol{y}) = \sum\nolimits_{i\in\mathcal{B}} \phi_i^d(\boldsymbol{y}_i) = \sum\nolimits_{i\in\mathcal{B}} \delta \exp\left(\beta \frac{\rho_i^d}{\rho_i^g}\right) \quad (23)$$

where β represents the network sensitivity towards DL on-grid power consumption ($\beta > 0$) and δ aims to adjust the value of cost function ($\delta > 0$). Figure 3 shows the curves of cost function of DL on-grid power consumption versus ρ_i^d/ρ_i^g with different values of β and δ. It is shown that with proper values of β and δ, such as $\beta = 6$ and $\delta = 10^{-4}$, which we adopt in this paper, the cost function of DL on-grid power consumption has the following property: when $\rho_i^d/\rho_i^g > 1$, $\phi_i^d(\boldsymbol{y}_i)$ increases exponentially with the rise of ρ_i^d and when $0 < \rho_i^d/\rho_i^g < 1$, $\phi_i^d(\boldsymbol{y}_i)$ remains almost zero. Such a property encourages the good use of the green power harvested from renewable energy sources, in order to reduce DL on-grid power consumption. Note that if the harvested green power of BS i is smaller than its static power consumption, we will set $\rho_i^g = \varepsilon$. In this case, any traffic load will cause huge DL on-grid power consumption cost, thereby resulting in fewer users associated with BS i and even turning BS i into sleep mode with no associated users.

Without loss of generality, for the cost of overall UL power consumption of users, we just define $\phi^u(\boldsymbol{y}) = P^u$. The larger overall UL power consumption of users will incur larger cost.

4. PROPOSED USER ASSOCIATION ALGORITHM

In this section, we propose the user association algorithm, which achieves the global optimum in minimising the total system cost $f(\boldsymbol{y})$. The proposed user association algorithm is implemented in an iterative manner: BSs periodically measure and advertise their loads, and then users make user association decision based on the advertised information to minimise $f(\boldsymbol{y})$. The BS and user sides update iteratively until convergence. The proposed user association algorithm is totally distributed. Through the interaction between BSs and users may incur overhead on control information exchange, the proposed algorithm does not require any centralised computation, as such it will not incur algorithmic complexity issue here.

In order to guarantee convergence, we assume that spatial load distributions in the HetNets area are temporally stationary, and the time scale of users making user association decisions is faster than that of BSs advertising their loads. In this case, BSs advertise their load conditions after the system remains stationary. We also assume that the green power of every BS is constant during the period of determining user association. Such an assumption is feasible. From statistics in real networks [27], the green power generation rate varies over time but could be assumed almost constant during a certain period, for example, 1 h, which is definitely much larger than that of traffic request arrival and departure process, for example, typically less than several minutes [16].

Because $y_i(x) \in \{0,1\}$, $f(\boldsymbol{y})$ is not continuously differentiable. In order to derive the optimal user association algorithm, we relax the feasible set by letting $0 \leqslant y_i(x) \leqslant 1$; here, $y_i(x)$ that specifies the probability of user at location x is associated with BS i. As such, the relaxed feasible

set of user association is

$$\widehat{\mathcal{F}} = \Big\{\boldsymbol{y}|0 \leqslant \rho_i^d \leqslant 1-\varepsilon, 0 \leqslant \tilde{\rho_i^d} \leqslant 1-\varepsilon, \\ 0 \leqslant \rho_i^u \leqslant 1-\varepsilon, 0 \leqslant \tilde{\rho_i^u} \leqslant 1-\varepsilon, \\ \textstyle\sum_{i\in\mathcal{B}} y_i(x) = 1, 0 \leqslant y_i(x) \leqslant 1, \forall i, \forall x\Big\} \tag{24}$$

Lemma 1. *The relaxed feasible set of user association $\widehat{\mathcal{F}}$ is convex.*

Proof. This lemma can be proved by the fact that $\widehat{\mathcal{F}}$ is composed of any convex combination of the user association $\boldsymbol{y}$. □

Remark 1. Although we relax the original deterministic user association $\mathcal{F}$ to probabilistic user association $\tilde{\mathcal{F}}$, the proposed user association algorithm determines the optimal deterministic user association, where $y_i(x)$ will be either 0 or 1. This will be made clear in the proof of Theorems 1 and 2.

We define the time interval between two consecutive traffic load advertisements as an iteration. If the $\rho_i^{d,(k)}$, $\tilde{\rho}_i^{d,(k)}$, $\rho_i^{u,(k)}$ and $\tilde{\rho}_i^{u,(k)}$ represent the DL traffic load, DL backhaul traffic load, UL traffic load and UL backhaul traffic load of BS i at kth iteration, respectively, and $y_i^{(k)}(x)$ is the user association indicator of user at location x at kth iteration, we can obtain

$$\frac{df(\boldsymbol{y})}{dy_i^{(k)}(x)} = \frac{\lambda(x)\mu(x)}{r_i^d(x)}\left(\pi_i^{d,(k)} + r_i^d(x)\tilde{\pi}_i^{d,(k)}\right) \\ + \frac{\lambda(x)\upsilon(x)}{r_i^u(x)}\left(\pi_i^{u,(k)} + r_i^u(x)\tilde{\pi}_i^{u,(k)}\right) \tag{25}$$

where

$$\pi_i^{d,(k)} = \left(1-\rho_i^{d,(k)}\right)^{-2} + \frac{\omega\beta\delta}{\rho_i^g}\exp\left(\beta\frac{\rho_i^{d,(k)}}{\rho_i^g}\right) \tag{26}$$

$$\tilde{\pi}_i^{d,(k)} = \left(1-\tilde{\rho}_i^{d,(k)}\right)^{-2}\left(R_i^d\right)^{-1} \tag{27}$$

$$\pi_i^{u,(k)} = \left(1-\rho_i^{u,(k)}\right)^{-2} + \omega\omega_p p_i^u(x) \tag{28}$$

$$\tilde{\pi}_i^{u,(k)} = \left(1-\tilde{\rho}_i^{u,(k)}\right)^{-2}\left(R_i^u\right)^{-1} \tag{29}$$

4.1. Procedure of the proposed user association algorithm

The proposed user association algorithm consists of two parts:

User side: During the kth iteration, users obtain the traffic loads $\rho_i^{d,(k)}$, $\tilde{\rho}_i^{d,(k)}$, $\rho_i^{u,(k)}$ and $\tilde{\rho}_i^{u,(k)}$, $\forall i \in \mathcal{B}$ of all the BSs via the broadcast. And then the user at location x chooses the optimal BS by

$$j^{(k)}(x) = \arg\max_{i\in\mathcal{B}} \\ \frac{r_i^d(x)r_i^u(x)}{\left(\pi_i^{d,(k)} + r_i^d(x)\tilde{\pi}_i^{d,(k)}\right)r_i^u(x) + \alpha(x)\left(\pi_i^{u,(k)} + r_i^u(x)\tilde{\pi}_i^{u,(k)}\right)r_i^d(x)} \tag{30}$$

where $\alpha(x) = \upsilon(x)/\mu(x)$, which is the ratio of UL and DL mean traffic size.

Then the user association indicator is updated by

$$\widehat{y}_i^{(k)}(x) = \begin{cases} 1, & \text{if } i = j^{(k)}(x) \\ 0, & \text{otherwise} \end{cases} \tag{31}$$

Based on the updated user association indicator, users broadcast their user association indicators to all the BSs as follows:

$$y_i^{(k+1)}(x) = (1-\varsigma)\,\widehat{y}_i^{(k)}(x) + \varsigma y_i^{(k)}(x) \tag{32}$$

where $0 \leqslant \varsigma < 1$ is the exponential averaging parameter.

BS side: The updated advertising user association indicators from the user side will change the loads of BSs, and then BS i updates the next advertising traffic load as follows:

$$\rho_i^{d,(k+1)} = \min\left(\int_{\mathcal{L}} \frac{\lambda(x)\mu(x)y_i^{(k+1)}(x)}{r_i^d(x)}dx, 1-\varepsilon\right) \tag{33}$$

$$\tilde{\rho}_i^{d,(k+1)} = \min\left(\int_{\mathcal{L}} \frac{\lambda(x)\mu(x)y_i^{(k+1)}(x)}{R_i^d}dx, 1-\varepsilon\right) \tag{34}$$

$$\rho_i^{u,(k+1)} = \min\left(\int_{\mathcal{L}} \frac{\lambda(x)\upsilon(x)y_i^{(k+1)}(x)}{r_i^u(x)}dx, 1-\varepsilon\right) \tag{35}$$

$$\tilde{\rho}_i^{u,(k+1)} = \min\left(\int_{\mathcal{L}} \frac{\lambda(x)\upsilon(x)y_i^{(k+1)}(x)}{R_i^u}dx, 1-\varepsilon\right) \tag{36}$$

4.2. Existence of optimal solution

Lemma 2. *A unique user association $\boldsymbol{y}*$ exists to minimise $f(\boldsymbol{y}) = \varphi(\boldsymbol{y}) + \omega\left(\phi^d(\boldsymbol{y}) + \phi^u(\boldsymbol{y})\right)$.*

Proof. The objective function $f(\boldsymbol{y})$ is a convex function of $\boldsymbol{y}$, when $\boldsymbol{y}$ is defined on $\widehat{\mathcal{F}}$, because $\nabla^2 f(\boldsymbol{y}) > 0$, when $\boldsymbol{y} \in \widehat{\mathcal{F}}$. As such, there exists a unique optimal $\boldsymbol{y}*$ that minimises $f(\boldsymbol{y})$. □

4.3. Convergence of the proposed user association algorithm

We denote $\widehat{y}^{(k)} = \left\{\widehat{y}_i^{(k)}|i\in\mathcal{B}\right\}$, where $\widehat{y}_i^{(k)} = \left\{\widehat{y}_i^{(k)}(x)|\widehat{y}_i^{(k)}(x) = \{0,1\}, x\in\mathcal{L}\right\}$, $\boldsymbol{y}^{(k)} = \left\{\boldsymbol{y}_i^{(k)}|i\in\mathcal{B}\right\}$, where $\boldsymbol{y}_i^{(k)} = \left\{y_i^{(k)}(x)|0 \leqslant y_i^{(k)}(x) \leqslant 1, x\in\mathcal{L}\right\}$.

Lemma 3. *When* $\widehat{y}^{(k)} \neq \boldsymbol{y}*$, $\widehat{y}^{(k)} - \boldsymbol{y}^{(k)}$ *is a descent direction of* $f(\boldsymbol{y}^{(k)})$.

Proof. This lemma can be proved by deriving $\left\langle \nabla f(\boldsymbol{y}^{(k)}), \widehat{y}^{(k)} - \boldsymbol{y}^{(k)} \right\rangle \leqslant 0$.

$$\begin{aligned}
&\left\langle \nabla f(\boldsymbol{y}^{(k)}), \widehat{\boldsymbol{y}}^{(k)} - \boldsymbol{y}^{(k)} \right\rangle \\
&= \int_{\mathcal{L}} \sum_{i\in\mathcal{B}} \left[\left(\lambda(x)\mu(x) \big/ r_i^d(x) \left(\pi_i^{d,(k)} + r_i^d(x)\tilde{\pi}_i^{d,(k)} \right) \right.\right. \\
&\quad \left. + \left(\lambda(x)\upsilon(x) \big/ r_i^u(x) \right) \left(\pi_i^{u,(k)} + r_i^u(x)\tilde{\pi}_i^{u,(k)} \right) \right) \\
&\quad \left. \times \left(\widehat{y}_i^{(k)}(x) - y_i^{(k)}(x) \right) \right] dx \\
&= \int_{\mathcal{L}} \lambda(x)\mu(x) \sum_{i\in\mathcal{B}} \left[\left(\left(\pi_i^{d,(k)} + r_i^d(x)\tilde{\pi}_i^{d,(k)} \right) \Big/ r_i^d(x) \right.\right. \\
&\quad \left. + \alpha(x) \left(\pi_i^{u,(k)} + r_i^u(x)\tilde{\pi}_i^{u,(k)} \right) \Big/ r_i^u(x) \right) \\
&\quad \left. \times \left(\widehat{y}_i^{(k)}(x) - y_i^{(k)}(x) \right) \right] dx
\end{aligned} \tag{37}$$

Note that Equation (38) holds, because $\widehat{y}_i^{(k)}(x)$ derived from Equations (30) and (31) maximises $\left[\left(\pi_i^{d,(k)} + r_i^d(x)\tilde{\pi}_i^{d,(k)} \right) r_i^d(x)^{-1} + \alpha(x) \left(\pi_i^{u,(k)} + r_i^u(x)\tilde{\pi}_i^{u,(k)} \right) r_i^u(x)^{-1} \right]^{-1}$, for all $i \in \mathcal{B}$. Hence, $\left\langle \nabla f(\boldsymbol{y}^{(k)}), \widehat{y}^{(k)} - \boldsymbol{y}^{(k)} \right\rangle \leqslant 0$. □

$$\sum_{i\in\mathcal{B}} \left(\frac{\left(\pi_i^{d,(k)} + r_i^d(x)\tilde{\pi}_i^{d,(k)} \right)}{r_i^d(x)} + \frac{\alpha(x)\left(\pi_i^{u,(k)} + r_i^u(x)\tilde{\pi}_i^{u,(k)} \right)}{r_i^u(x)} \right) \widehat{y}_i^{(k)}(x) \leqslant \sum_{i\in\mathcal{B}} \left(\frac{\left(\pi_i^{d,(k)} + r_i^d(x)\tilde{\pi}_i^{d,(k)} \right)}{r_i^d(x)} + \frac{\alpha(x)\left(\pi_i^{u,(k)} + r_i^u(x)\tilde{\pi}_i^{u,(k)} \right)}{r_i^u} (x) \right) y_i^{(k)}(x) \tag{38}$$

Theorem 1. *The user association* $\boldsymbol{y}$ *converges to* $\boldsymbol{y}^* \in \mathcal{F}$ *that minimises* $f(\boldsymbol{y})$.

Proof. Because of $y_i^{(k+1)}(x) - y_i^{(k)}(x) = (1-\zeta)\,\widehat{y}_i^{(k)}(x) + \zeta y_i^{(k)}(x) - y_i^{(k)}(x) = (1-\zeta)\left(\widehat{y}_i^{(k)}(x) - y_i^{(k)}(x) \right)$ and $0 \leqslant \zeta < 1$, $\boldsymbol{y}^{(k+1)} - \boldsymbol{y}^{(k)}$ is also a descent direction of $f\left(\boldsymbol{y}^{(k)}\right)$ according to Lemma 3. Based on Lemma 2 where $f\left(\boldsymbol{y}^{(k)}\right)$ is a convex function and is lower bounded by 0, we conclude that $f\left(\boldsymbol{y}^{(k)}\right)$ converges. Suppose that $f\left(\boldsymbol{y}^{(k)}\right)$ converges to some point other than $f(\boldsymbol{y}^*)$, then $\boldsymbol{y}^{(k+1)}$ produces a descent direction again, which means that $f\left(\boldsymbol{y}^{(k)}\right)$ can further decrease in the next iteration. This contradicts the convergence assumption. As such, $\boldsymbol{y}^{(k)}$ converges to $\boldsymbol{y}^*$. Because $\boldsymbol{y}^{(k)}$ is derived based on Equations (30)–(36), where $\widehat{y}_i^{(k)}(x) = \{0,1\}$, $\boldsymbol{y}^*$ is in the feasible set $\mathcal{F}$. □

4.4. Optimality of the proposed user association algorithm

Theorem 2. *Suppose that the user association problem is feasible, the deterministic user association* $\boldsymbol{y}* = \left\{ \boldsymbol{y}_i^* | i \in \mathcal{B} \right\}$, *where* $\boldsymbol{y}_i{}^* = \{ y_i{}^*(x) | y_i{}^*(x) = \{0,1\}, x \in \mathcal{L} \}$, *is the optimal solution to the user association problem.*

Proof. Because $f(\boldsymbol{y})$ is a convex function over a convex set $\widehat{\mathcal{F}}$, if $\boldsymbol{y}_i{}^*$ satisfies the following conditions,

$$\left\langle \nabla f\left(\boldsymbol{y}^*\right),\ \boldsymbol{y} - \boldsymbol{y}^* \right\rangle \geqslant 0 \tag{39}$$

for all $\boldsymbol{y} \in \widehat{\mathcal{F}} \backslash \boldsymbol{y}^*$, then $\boldsymbol{y}^*$ is the optimal solution for the user association problem.

Based on Equations (30)–(32) and Theorem 1, we can conclude that the converged user association is deterministic, that is,

$$y_i^*(x) = \mathbf{1}\left\{ i = j^*(x) \right\} \tag{40}$$

where

$$j^*(x) = \arg\max_{i\in\mathcal{B}} \frac{r_i^d(x) r_i^u(x)}{\left(\pi_i^{d,*} + r_i^d(x)\tilde{\pi}_i^{d,*} \right) r_i^u(x) + \alpha(x)\left(\pi_i^{u,*} + r_i^u(x)\tilde{\pi}_i^{u,*} \right) r_i^d(x)} \tag{41}$$

And then the inner product can be computed as follows:

$$\begin{aligned}
&\langle \nabla f(\boldsymbol{y}^*), \boldsymbol{y} - \boldsymbol{y}^* \rangle \\
&= \int_{\mathcal{L}} \sum_{i\in\mathcal{B}} \left[\left(\lambda(x)\mu(x) \big/ r_i^d(x) \left(\pi_i^{d,*} + r_i^d(x)\tilde{\pi}_i^{d,*} \right) \right.\right. \\
&\quad \left. + \left(\lambda(x)\upsilon(x) \big/ r_i^u(x) \right) \left(\pi_i^{u,*} + r_i^u(x)\tilde{\pi}_i^{u,*} \right) \right) \\
&\quad \left. \times (y_i(x) - y_i{}^*(x)) \right] dx \\
&= \int_{\mathcal{L}} \lambda(x)\mu(x) \sum_{i\in\mathcal{B}} \left[\left(\left(\pi_i^{d,*} + r_i^d(x)\tilde{\pi}_i^{d,*} \right) \Big/ r_i^d(x) \right.\right. \\
&\quad \left. + \alpha(x) \left(\pi_i^{u,*} + r_i^u(x)\tilde{\pi}_i^{u,*} \right) \Big/ r_i^u(x) \right) \\
&\quad \left. \times (y_i(x) - y_i{}^*(x)) \right] dx
\end{aligned} \tag{42}$$

Note that

$$\begin{aligned}
&\sum_{i\in\mathcal{B}} \left(\frac{\left(\pi_i^{d,*} + r_i^d(x)\tilde{\pi}_i^{d,*} \right)}{r_i^d(x)} + \frac{\alpha(x)\left(\pi_i^{u,*} + r_i^u(x)\tilde{\pi}_i^{u,*} \right)}{r_i^u(x)} \right) y_i(x) \\
&\geqslant \sum_{i\in\mathcal{B}} \left(\frac{\left(\pi_i^{d,*} + r_i^d(x)\tilde{\pi}_i^{d,*} \right)}{r_i^d(x)} + \frac{\alpha(x)\left(\pi_i^{u,*} + r_i^u(x)\tilde{\pi}_i^{u,*} \right)}{r_i^u(x)} \right) y_i{}^*(x)
\end{aligned} \tag{43}$$

holds, and thus, $\langle \nabla f(\boldsymbol{y}^*),\ \boldsymbol{y} - \boldsymbol{y}^* \rangle \geqslant 0$. Therefore, the deterministic user association $\boldsymbol{y}*$ is the optimal solution of the user association problem. □

Remark 2. The optimisation problem (20) is combinational because of the binary variable $y_i(x)$. The complexity

of the centralised brute-force algorithm is $\mathcal{O}\left(|\mathcal{B}|^{|\mathcal{U}|}\right)$, with $|\mathcal{U}|$ denoted as the total number of users in the HetNets area at one time. Such complexity is impossible even for a modest-sized network. Furthermore, centralised algorithm requires global network information and centralised controller for coordination, and the amount of exchanged information is proportional to $(|\mathcal{B}| \times |\mathcal{U}|)$. On the contrary, the computational complexity of the proposed distributed user association algorithm for an individual user is $\mathcal{O}(|\mathcal{B}|)$ in each iteration. As for the exchanged information, in each iteration, each BS broadcasts ρ_i^d, $\tilde{\rho_i^d}$, ρ_i^u and $\tilde{\rho_i^u}$, and each user feedbacks its association request only to the chosen BS. Thus, the exchanged information in the proposed distributed algorithm is $(|\mathcal{B}| + |\mathcal{U}|)$ for each iteration. According to [17], although the convergence speed depends on the value of exponential averaging parameter ς, fixed ς close to 1 generally works well for the convergence. However, how to optimise ς is beyond the scope of this paper. In our simulation, we set $\varsigma = 0.98$; simulation results have shown that our proposed user association algorithm converges quickly to the optimum, within 150 iterations.

Remark 3. Up till now, we consider the condition where the optimisation problem (20) is feasible, that is, the feasible set $\mathcal{F}$ is not empty with $\rho_i^d \leqslant 1-\varepsilon$, $\tilde{\rho_i^d} \leqslant 1-\varepsilon, \rho_i^u \leqslant 1-\varepsilon$, $\tilde{\rho_i^u} \leqslant 1-\varepsilon$, $\forall i \in \mathcal{B}$. However, in the circumstance when the optimisation problem (20) is not feasible because of high traffic load, the admission control is required. In this case, the admission control with the objective to minimise the sum cost of average traffic delay, power consumption and blocking traffic can be formulated with the similar approach in our previous work [18], where a threshold is used to determine whether a particular user should be blocked or not, and the user association algorithm stays intact as the algorithm presented earlier in this section.

5. SIMULATION RESULTS

To evaluate the performance of the proposed user association algorithm (proposed joint UL–DL UA), we simulate a HetNet composed of 19 macrocells. In each macrocell, six PBSs are symmetrically located along a circle with radius as 200 m and MBS in the centre. We assume that the green power of every BS is constant during a snapshot of simulation. As for the traffic model, for the sake of simplicity, we simulate that the file transfer requests follow a homogenous Poisson point process where $\lambda(x) = \lambda$, but note that our model can still apply to the scenario with heterogeneous traffic distributions. In the simulation, we assume that each BS has the same UL and DL backhaul data rate. Without specific indication, the backhaul data rates of MBS and PBS are defined as 100 and 60 Mbps, respectively [28]. Each UL and DL request is assumed to have exactly one file with mean file size υ as 80 Kbits and μ as 100 Kbits, as generally there is more traffic in DL than that in UL. As we adopt TDD to separate UL and DL transmissions, there is channel reciprocity between UL and DL transmissions.

The other simulation parameters are shown in Table I.

We first set the weight ω between cost of average traffic delay and power consumption as 10^{-1}, and the traffic arrival rate as 1.2. Figure 4 compares the snapshot of the resulting user association pattern in one macrocell area in different scenarios with different distributions of green power harvested from renewable energy sources as defined in Table II. In scenario 2, the green powers of all the PBSs are the same as those in scenario 1, except that the green power of MBS is lower than that in scenario 1. Figure 4 shows that compared with scenario 2, more users are associated with MBS in scenario 1, where MBS has larger green power. This figure indicates that the proposed algorithm is able to adapt the traffic loads among BSs along with the distribution of green power, in order to make good use of the renewable energy and reduce DL on-grid power consumption. In scenario 3, the green power of

Table I. Simulation parameters.

Parameter	Value
Bandwidth	10 MHz
Inter-site distance	500 m
Transmission power of MBS	46 dBm
Transmission power of PBS	30 dBm
Maximum transmission power of user	23 dBm
Noise power	−174 dBm/Hz
Weight of UL/DL power consumption ω_p	100
Pathloss between MBS and user	$128.1 + 37.6\log_{10} d$ (km) [29]
Pathloss between PBS and user	$140.7 + 36.7\log_{10} d$ (km) [29]
Log-normal shadowing fading	10 dB [29]
Static power consumption of MBS	780 W [25]
Static power consumption of PBS	13.6 W [25]
Slope of MBS load-dependent power	4.7 [25]
Slope of PBS load-dependent power	4.0 [25]

DL, downlink; UL, uplink; BS, base station; MBS, macro-BS; PBS, pico BS.

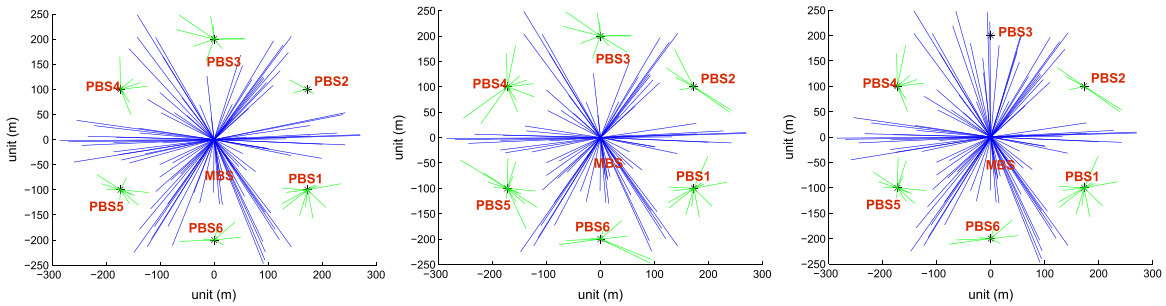

(a) Scenario 1 (b) Scenario 2 (c) Scenario 3

Figure 4. Snapshot of user association pattern: scenarios (a) 1, (b) 2 and (c) 3. BS, base station; MBS, macro BS; PBS, pico BS.

Table II. Green power distribution in different scenarios.

Scenario	MBS (W)	PBS1 (W)	PBS2 (W)	PBS3 (W)	PBS4 (W)	PBS5 (W)	PBS6 (W)
1	974	33	32	33	31	32	33
2	870	33	32	33	31	32	33
3	870	33	32	10	31	32	33

BS, base station; MBS, macro BS; PBS, pico BS.

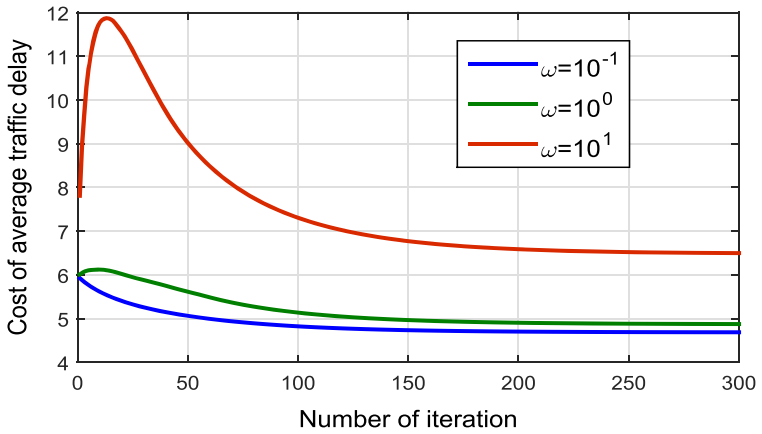

Figure 5. Cost of average traffic delay versus different numbers of iteration.

PBS3 is 10 W, which is lower than the static power consumption. We can observe from Figure 4(c) that there is no user associated with PBS3, leading to PBS3 switched into sleep mode. As such, our proposed algorithm is capable of controlling the BS on/off dynamically according to the available amount of green power, thereby undisputedly reducing the DL on-grid power consumption effectively.

In the following simulation, we evaluate the performance of the proposed joint UL–DL UA in scenario 2.

Figures 5 and 6 demonstrate the cost of average traffic delay $\varphi(\boldsymbol{y})$ and cost of power consumption $\left(\phi^d(\boldsymbol{y})+\phi^u(\boldsymbol{y})\right)$ with different values of weight ω, respectively. We can observe that with the increase of weight ω, the cost of average traffic delay rises and the cost of power consumption decreases. The larger weight ω will lead to more emphasis on the power saving in order to minimise DL on-grid power consumption and overall UL power consumption of users, while the smaller weight ω will attach more importance to the average traffic delay minimisation. This figure indicates that the weight ω in the proposed joint UL–DL UA could adjust the trade-off between average traffic delay and power consumption. Note that such trade-off graph may also be used to choose the value of ω in practice based on the maximum tolerable traffic delay. From Figures 5 and 6, we can also obtain the convergence of the proposed joint UL–DL UA. It is shown that the proposed algorithm converges quickly to the global optimum within less than 150 iterations.

In the subsequent simulation, we set $\omega = 10^{-1}$. In order to better benchmark the performance of the proposed joint UL–DL UA, we also implement two baseline algorithms: the max RSRP user association (max RSRP UA) and the user association for DL delay-power trade-off (DL-only UA). Max RSRP UA is the conventional user association

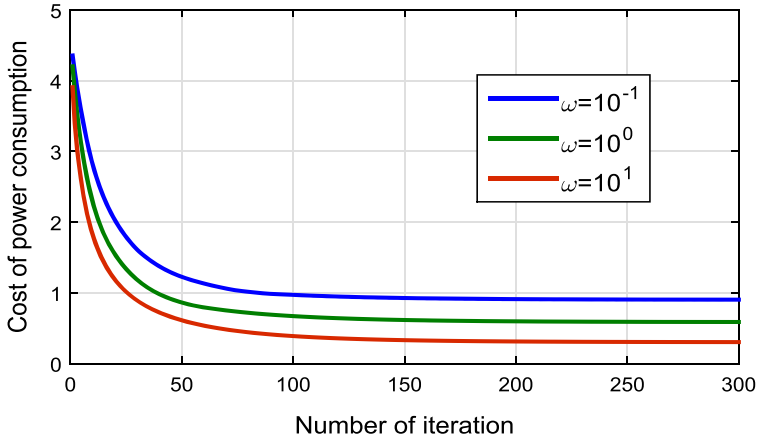

Figure 6. Cost of power consumption versus different numbers of iteration.

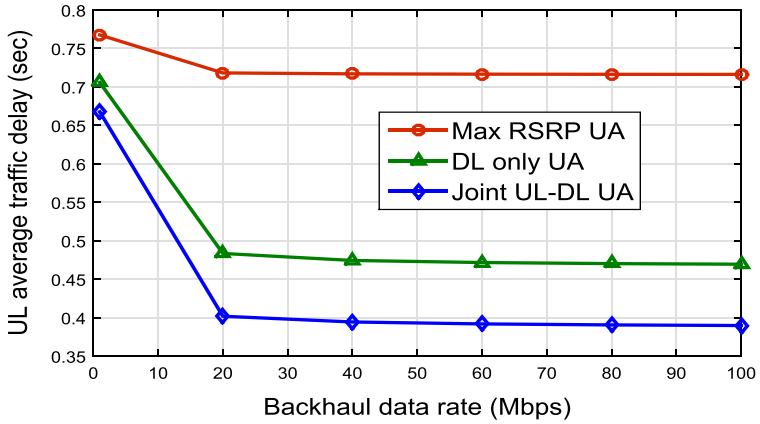

Figure 7. UL average traffic delay versus different pico BS backhaul data rates. UL, uplink; DL, downlink; RSRP, reference signal received power; max RSRP UA, max RSRP user association; DL-only UA, user association for DL delay-power trade-off; joint UL–DL UA, proposed user association algorithm.

policy, where a user will associate with the BS from which it receives the highest RSRP. In DL-only UA, user association is determined to achieve the trade-off between DL average traffic delay and DL on-grid power consumption without considering the UL transmission, or equivalently, the DL-only UA aims to minimise the system cost, which is given by

$$f(\boldsymbol{y}) = \sum\nolimits_{i\in\mathcal{B}} \left(\tau_i^d(\boldsymbol{y}) + \tilde{\tau_i^d}(\boldsymbol{y})\right) + \omega\phi^d(\boldsymbol{y}) \qquad (44)$$

Figures 7–10 compare the performance of these three algorithms with different backhaul data rates of PBS. Figures 7 and 8 show the UL and DL average traffic delay, including both the wireless access and backhaul delays, and different backhaul data rates of PBS, respectively. Both the UL and DL average traffic delays decrease with the increase of PBS backhaul rate. When the backhaul data rate of PBS is very small, say 1 Mbps in our simulation, the average traffic delay differences of these three algorithms are not distinct. This is because PBSs are easily congested by relatively light traffic load, due to the low backhaul data rate. In this sense, because both the DL-only UA and proposed joint UL–DL UA are backhaul aware, they will associate fewer users with PBSs in order to avoid PBS congestion, thereby achieving the similar effect with the max RSRP UA, which associates most of users with the macrocell due to the transmission power disparity between MBS and PBS. However, with the increase of PBS backhaul data rate, the backhaul data rate is no longer the bottleneck. As such, both the backhaul-aware DL-only UA and proposed joint UL–DL UA are able to offload more users from macrocells, achieving much less average traffic delay than that of max RSRP UA. We can also observe from Figures 7 and 8 that the proposed joint UL–DL UA is superior to the DL-only UA in terms of UL average traffic delay but obtains inferior DL average traffic delay. It can be explained by the fact that with the consideration on both UL and DL transmissions, the proposed joint UL–DL UA trades the DL average traffic delay for the UL average traffic delay, to achieve the optimal overall delay reduction.

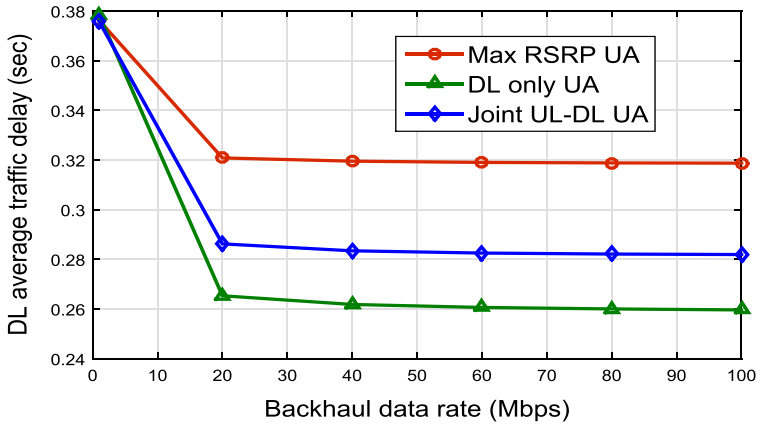

Figure 8. DL average traffic delay versus different pico BS backhaul data rates. UL, uplink; DL, downlink; RSRP, reference signal received power; max RSRP UA, max RSRP user association; DL-only UA, user association for DL delay-power trade-off; joint UL–DL UA, proposed user association algorithm.

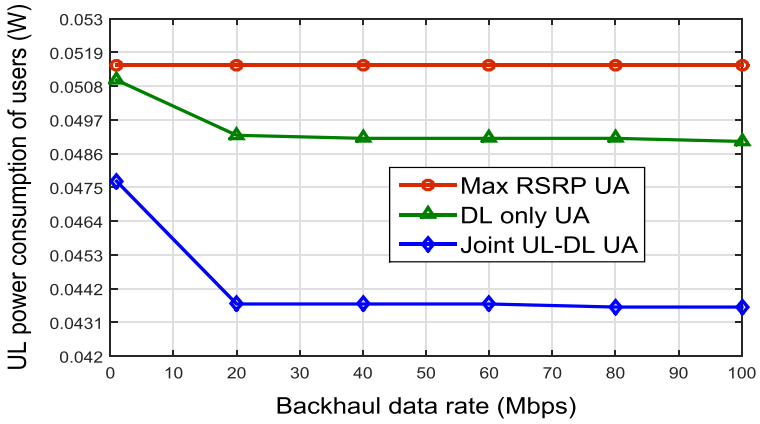

Figure 9. Overall UL power consumption of users versus different pico BS backhaul data rates. UL, uplink; DL, downlink; RSRP, reference signal received power; max RSRP UA, max RSRP user association; DL-only UA, user association for DL delay-power trade-off; joint UL–DL UA, proposed user association algorithm.

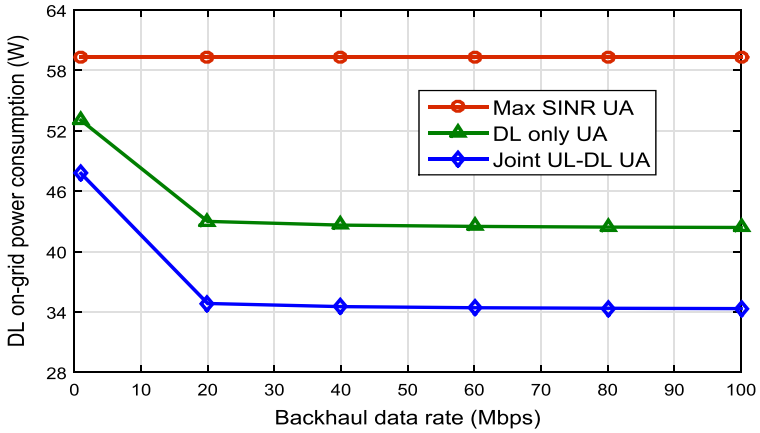

Figure 10. DL on-grid power consumption versus different pico BS backhaul data rates. UL, uplink; DL, downlink; RSRP, reference signal received power; max RSRP UA, max RSRP user association; DL-only UA, user association for DL delay-power trade-off; joint UL–DL UA, proposed user association algorithm; SINR, signal-to-interference-plus-noise ratio.

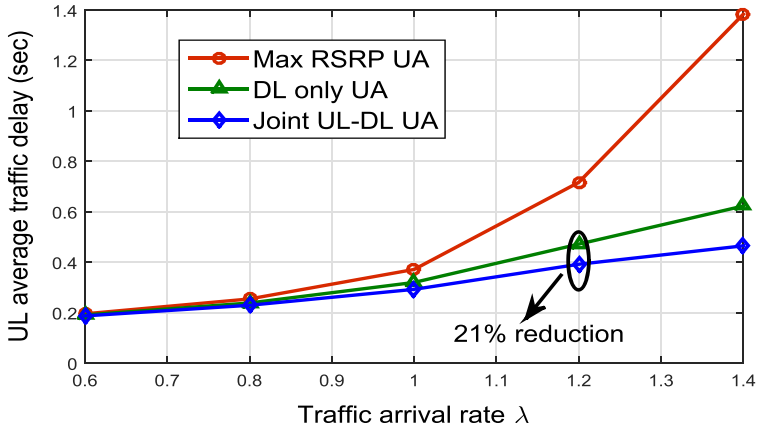

Figure 11. UL average traffic delay versus different traffic arrival rates. UL, uplink; DL, downlink; RSRP, reference signal received power; max RSRP UA, max RSRP user association; DL-only UA, user association for DL delay-power trade-off; joint UL–DL UA, proposed user association algorithm.

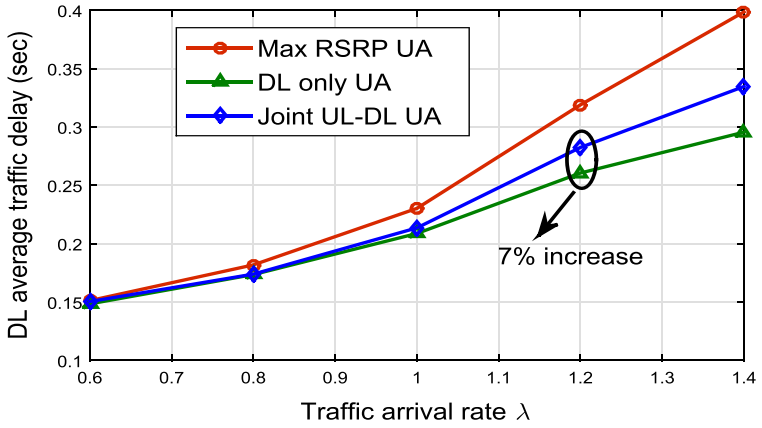

Figure 12. DL average traffic delay versus different traffic arrival rates. UL, uplink; DL, downlink; RSRP, reference signal received power; max RSRP UA, max RSRP user association; DL-only UA, user association for DL delay-power trade-off; joint UL–DL UA, proposed user association algorithm.

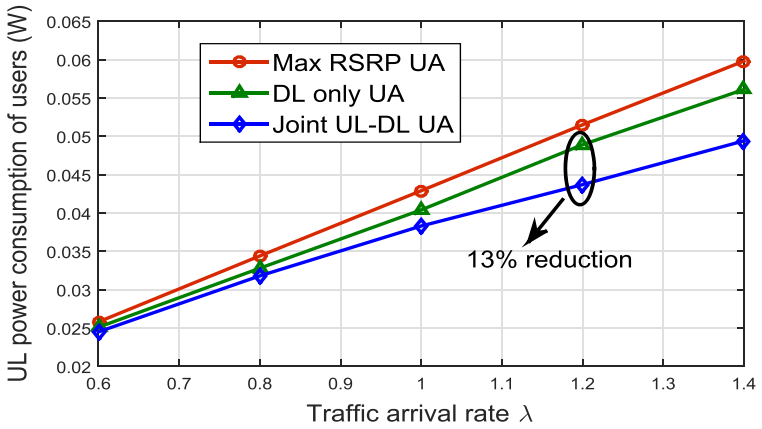

Figure 13. Overall UL power consumption of users versus different traffic arrival rates. UL, uplink; DL, downlink; RSRP, reference signal received power; max RSRP UA, max RSRP user association; DL-only UA, user association for DL delay-power trade-off; joint UL–DL UA, proposed user association algorithm.

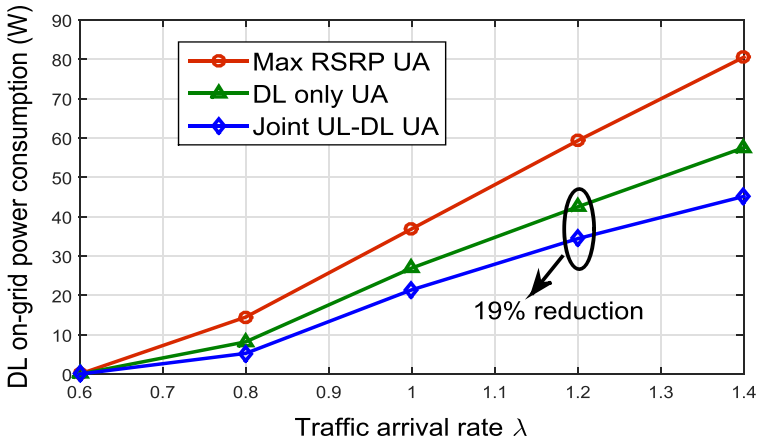

Figure 14. DL on-grid power consumption versus different traffic arrival rates. UL, uplink; DL, downlink; RSRP, reference signal received power; max RSRP UA, max RSRP user association; DL-only UA, user association for DL delay-power trade-off; joint UL–DL UA, proposed user association algorithm.

Figures 9 and 10 show the overall UL power consumption of users and DL on-grid power consumption versus different backhaul data rates of PBS, respectively. The DL on-grid power consumption that we plotted here is the sum DL on-grid power consumption of all the BSs in one marcocell area. For max RSRP UA, both the overall UL power consumption of users and DL on-grid power consumption do not change with the PBS backhaul data rate, because max RSRP UA does not take backhaul data rate as a metric when making the user association decision. For both the DL-only UA and proposed joint UL–DL UA, the overall UL power consumption of users and DL on-grid power consumption decrease with the increment of the backhaul data rate of PBS. With larger PBS backhaul data rate, more users will be offloaded from the congested macrocell, resulting in the load balancing and power saving throughout the whole network. We also obtain an interesting observation that the proposed joint UL–DL UA outperforms the DL-only UA in terms of both the overall UL power consumption and DL on-grid power consumption reductions.

Figures 7–10 also demonstrate that when the PBS backhaul data rate exceeds some point (20 Mbps in our simulation), the UL and DL average traffic delays change slightly with the increase of PBS backhaul data rate, and the DL on-gird power consumption and UL power consumption stay almost the same with the rise of PBS backhaul data rate. This is because when the PBS backhaul data rate is large enough, it is no longer the bottleneck for network performance. As such, the increase of PBS backhaul data rate will not affect the resulting user association pattern.

Finally, Figures 11–14 compare the performance of these three algorithms with different traffic arrival rates. Figures 11, 12, 13 and 14 demonstrate the UL average traffic delay, DL average traffic delay, overall UL power consumption of users and DL on-grid power consumption versus different traffic arrival rates, respectively. It is easy to understand that the increasing traffic arrival rate will bring in larger average traffic delay and more power consumption. Whatever the traffic arrival rate is, the proposed joint UL–DL UA achieves comparable DL average traffic delay compared with the DL-only UA while effectively reducing the UL average traffic delay, achieving DL on-grid power conservation and saving the overall UL power consumption of users.

6. CONCLUSIONS

In this paper, we have proposed an optimal backhaul-aware joint UL and DL user association for delay-power trade-offs in HetNets with hybrid energy sources, where all the BSs are assumed to be powered by both the power grid and renewable energy sources. With the convex optimisation problem formulation, we have proved that the proposed user association algorithm converges to the global optimum, which minimises the weighted sum of cost of average traffic delay and cost of power consumption. The proposed user association algorithm allows for a flexible trade-off between average traffic delay and power consumption by adjusting the value of weight ω. Simulation results demonstrate that the proposed algorithm is capable of adapting the loads of BSs along with the distribution of green power and the PBS backhaul data rate, thereby effectively reacting to random green power availability in BSs and PBS backhaul constraints. Simulation results also validate the merits of the proposed user association algorithm in not only effectively reducing UL average traffic delay, overall UL power consumption of users and DL on-grid power consumption but also achieving comparable DL average traffic delay, compared with the user association algorithm only based on DL performance.

REFERENCES

1. Hoadley J, Maveddat P. Enabling small cell deployment with HetNet. *IEEE Wireless Communications* 2012; **19**(2): 4–5.
2. Ng D, Lo E, Schober R. Energy-efficient resource allocation in OFDMA systems with hybrid energy harvesting base station. *IEEE Transactions on Wireless Communications* 2013; **12**(7): 3412–3427.
3. Gong J, Zhou S, Niu Z. Optimal power allocation for energy harvesting and power grid coexisting wireless communication systems. *IEEE Transactions on Communications* 2013; **61**(7): 3040–3049.
4. Cui Y, Lau V, Wu Y. Delay-aware BS discontinuous transmission control and user scheduling for energy harvesting downlink coordinated MIMO systems. *IEEE Transactions on Signal Processing* 2012; **60** (7): 3786–3795.
5. Zheng M, Pawelczak P, Stanczak S, Yu H. Planning of cellular networks enhanced by energy harvesting. *IEEE Communications Letters* 2013; **17**(6): 1092–1095.
6. Liu D, Chen Y, Chai KK, Zhang T, Han K. Joint user association and green energy allocation in HetNets with hybrid energy sources. In *Proceedings of the 2015 IEEE Wireless Communications and Networking Conference (WCNC)*, New Orleans, LA, USA, 2015; 1542–1547.
7. Liu D, Chen Y, Chai KK, Zhang T. Optimal user association for delay-power tradeoffs in HetNets with hybrid energy sources. In *Proceedings of the 2014 IEEE 25th Annual International Symposium on Personal, Indoor and Mobile Radio Communication (PIMRC)*, Washington, DC, USA, 2014; 1857–1861.
8. Qian LP, Zhang YJ, Wu Y, Chen J. Joint base station association and power control via benders' decomposition. *IEEE Transactions on Wireless Communications* 2013; **12**(4): 1651–1665.
9. Liu D, Chen Y, Chai KK, Zhang T, Elkashlan M. Opportunistic user association for multi-service HetNets using Nash bargaining solution. *IEEE Communications Letters* 2014; **18**(3): 463–466.
10. Saad W, Han Z, Zheng R, Debbah M, Poor H. A college admissions game for uplink user association in wireless small cell networks. In *Proceedings of the 2014 IEEE INFOCOM*, Toronto, Canada, 2014; 1096–1104.
11. Yan S, Wang W, Zhao Z, Ahmed A. Investigation of cell association techniques in uplink cloud radio access networks. *Transactions on Emerging Telecommunications Technologies* 2014. DOI: 10.1002/ett.2894.
12. Lopez-Perez D, Chu X, Guvenc I. On the expanded region of picocells in heterogeneous networks. *IEEE Journal of Selected Topics in Signal Processing* 2012; **6**(3): 281–294.
13. Liu D, Chen Y, Chai KK, Zhang T. Joint uplink and downlink user association for energy-efficient HetNets using Nash bargaining solution. In *Proceedings of the 2014 IEEE 79th Vehicular Technology Conference (VTC Spring)*, Seoul, Korea, 2014; 1–5.
14. Luo S, Zhang R, Lim TJ. Downlink and uplink energy minimization through user association and beamforming in C-RAN. *IEEE Transactions on Wireless Communications* 2015; **14**(1): 494–508.
15. Nakamura T, Nagata S, Benjebbour A, Kishiyama Y, Hai T, Xiaodong S, Ning Y, Nan L. Trends in small cell enhancements in LTE advanced. *IEEE Communications Magazine* 2013; **51**(2): 98–105.
16. Son K, Kim H, Yi Y, Krishnamachari B. Base station operation and user association mechanisms for energy-delay tradeoffs in green cellular networks. *IEEE Journal on Selected Areas in Communications* 2011; **29**(8): 1525–1536.
17. Kim H, de Veciana G, Yang X, Venkatachalam M. Distributed alpha-optimal user association and cell load balancing in wireless networks. *IEEE/ACM Transactions on Networking* 2012; **20**(1): 177–190.
18. Liu D, Chen Y, Chai KK, Zhang T. Distributed delay-energy aware user association in 3-tier HetNets with hybrid energy sources. In *Proceedings of the 2014 Globecom Workshops (GC Wkshps)*, Austin, TX USA, 2014; 1109–1114.
19. Xu H, Zhang T, Zeng Z, Liu D. Distributed user association for delay-load tradeoffs in energy harvesting enabled HetNets. In *Proceedings of the 2015 IEEE Wireless Communications and Networking Conference Workshops (WCNCW)*, New Orleans, LA, USA, 2015; 386–390.
20. Niyato D, Lu X, Wang P. Adaptive power management for wireless base stations in a smart grid environment. *IEEE Wireless Communications* 2012; **19**(6): 44–51.
21. Shen Z, Khoryaev A, Eriksson E, Pan X. Dynamic uplink-downlink configuration and interference management in TD-LTE. *IEEE Communications Magazine* 2012; **50**(11): 51–59.
22. Chen X, Hu R. Joint uplink and downlink optimal mobile association in a wireless heterogeneous network. In *Proceedings of the 2012 IEEE Global Communications Conference (GLOBECOM)*, Anaheim, CA, USA, 2012; 4131–4137.
23. Pantisano F, Bennis M, Saad W, Debbah M. Cache-aware user association in backhaul-constrained small cell networks. In *12th International Symposium on Modeling and Optimization in Mobile, Ad Hoc, and Wireless Networks (WiOpt)*, Hammamet, Tunisia, 2014; 37–42.
24. Goiri In, Le K, Nguyen TD, Guitart J, Torres J, Bianchini R. Greenhadoop: leveraging green energy in data-processing frameworks. In *Proceedings of the 7th ACM European Conference on Computer Systems*, Bern, Switzerland, 2012; 57–70.
25. Auer G, Giannini V, Desset C, Godor I, Skillermark P, Olsson M, Imran M, Sabella D, Gonzalez M, Blume O,

Fehske A. How much energy is needed to run a wireless network? *IEEE Wireless Communications* 2011; **18**(5): 40–49.
26. Walrand J. *An Introduction to Queueing Networks*. Prentice-Hall: Upper Saddle River, NJ, 1998.
27. NREL. *Pvwatts*. Available from: http://rredc.nrel.gov/solar/calculators/pvwatts/version1/ [3 March 2015].
28. Networks C. Wireless backhaul solutions for small cells 2014. Available from: https://www.ceragon.com/images/Reasource_Center/Solution_Briefs/Ceragon_Solution_Brief_Wireless_Backhaul_Solutions_for_Small_Cells.pdf.
29. 3GPP. Further Advancements for E-UTRA Physical Layer Aspects (TR 36.814), 2010.